applied sciences

MDPI

Article

Synchronization and Application of a Novel Hyperchaotic System Based on Adaptive Observers

Erman Ozpolat [1,*] and Arif Gulten [2]

[1] Department of Electrical-Electronics Engineering, Mus Alparslan University, Mus 49100, Turkey
[2] Department of Electrical-Electronics Engineering, Firat University, Elazig 23119, Turkey
* Correspondence: e.ozpolat@alparslan.edu.tr; Tel.: +90-436-249-49-49

Abstract: This paper explores the synchronization and implementation of a novel hyperchaotic system using an adaptive observer. Hyperchaotic systems, known for possessing a greater number of positive Lyapunov exponents compared to chaotic systems, present unique challenges and opportunities in control and synchronization. In this study, we introduce a novel hyperchaotic system, thoroughly examining its dynamic properties and conducting a comprehensive phase space analysis. The proposed hyperchaotic system undergoes validation through circuit simulation to confirm its behavior. Introducing an adaptive observer synchronization technique, we successfully synchronize the dynamics of the novel hyperchaotic system with an identical counterpart. Importantly, we extend the application of this synchronization method to the domain of secure communication, showcasing its practical usage. Simulation outcomes validate the effectiveness of our methodology, demonstrating favorable results in the realm of adaptive observer-based synchronization. This research contributes significantly to the understanding and application of hyperchaotic systems, offering insights into both the theoretical aspects and practical implementation. Our findings suggest potential advancements in the field of chaotic systems, particularly in their applications within secure communication systems. By presenting motivations, methods, results, conclusions and the significance of our work in a more appealing manner, we aim to engage readers and highlight the innovative contributions of this study.

Keywords: hyperchaotic systems; adaptive observers; synchronization; secure communication

Citation: Ozpolat, E.; Gulten, A. Synchronization and Application of a Novel Hyperchaotic System Based on Adaptive Observers. *Appl. Sci.* **2024**, *14*, 1311. https://doi.org/10.3390/app14031311

Academic Editor: Alessandro Lo Schiavo

Received: 12 January 2024
Revised: 30 January 2024
Accepted: 1 February 2024
Published: 5 February 2024

1. Introduction

The understanding of chaotic behavior was greatly advanced in the 1960s when Edward Lorenz developed a computer program to simulate airflow, which is when chaos theory first emerged [1]. Extensive study was conducted in the 1970s when Lorenz discovered that even minimal changes in the initial circumstances might have a significant influence on weather forecasts. According to this study, system states varied significantly based on the basic characteristic of chaotic systems, which is the smallest deviation between two beginning circumstances [2].

The study of hyperchaotic systems was further developed in 1979 when Rössler discovered a four-dimensional hyperchaotic system [3]. Multidimensional chaotic and hyperchaotic systems became more well-known in the following years, providing useful applications in science and engineering [4]. Recently, there are many studies to be found in the literature on the dynamic analysis of chaotic systems [5–7].

In contrast to chaotic systems, hyperchaotic systems, which have multiple positive Lyapunov exponents, are more unpredictable and resistant to control. This property has drawn interest from the encryption and communication industries [8]. Multiple attractors improve security by making it more difficult for an attacker to determine the precise state of the system, which makes hyperchaotic systems more resistant to disruptions [9]. Secure applications of hyperchaotic systems have been a topic of great interest recently [10,11].

Circuit simulations of hyperchaotic systems facilitate real-world exploration and analysis of their dynamics, validating theoretical models and providing insights into system behavior under different conditions [12,13]. The implementation of hyperchaotic systems in circuits offers practical applications in secure communications, random number generation and nonlinear dynamics research [14,15].

Synchronization has gained attention in the context of hyperchaotic systems, especially with the growing focus on secure communication applications [16]. In order to attain coherence, synchronization entails changing the dynamic behaviors of two systems, referred to as the driver and reaction [17]. In an effort to compel the response system to synchronize with the driving system, the notion of synchronization in chaotic systems was first presented in 1990 [18]. To this end, a number of approaches have been put forth, such as adaptive design techniques and sampled data feedback synchronization [19,20].

Observer-based hyperchaotic system synchronization involves designing an observer (state estimator) and control strategy to achieve synchronization between two or more hyperchaotic systems [21]. Observers play a crucial role in estimating unmeasurable states, overcoming challenges posed by limited sensors or measurements, especially in hyperchaotic systems. Adaptive observers address uncertainties and variations in system parameters, enhancing the robustness and effectiveness of synchronization strategies [22].

The synchronization of adaptive observer-based hyperchaotic systems holds particular importance in secure communication systems [23]. The complex dynamics of hyperchaotic systems offer potential for encryption. Decryption and synchronization of these systems are vital for establishing secure communication channels [24]. The inclusion of adaptive observers adds robustness to the synchronization process, addressing uncertainties and variations in real-world applications [25].

The synchronization and implementation of adaptive observer-based hyperchaotic systems present a promising approach for secure communication. This approach, encompassing dynamic encryption keys, adaptation to changing conditions and resistance to attacks, proves valuable for applications where secure and robust communication is imperative. Typical examples are military communications, financial transactions, or confidential data transfer [26].

Xiong et al. [27] proposed a new 4-dimensional hyperchaotic system. They synchronized the proposed system with a reduced number of amplifiers. This synchronization has been used in secure communication applications. Zhang et al. [15] proposed a 4-dimensional hyperchaotic system based on cosine function. The authors have demonstrated the dynamic analysis and synchronization of the new system. They also presented an FPGA-based implementation of their proposed hyperchaotic system. Iskakova et al. [28] proposed a new nonlinear 4-dimensional hyperchaotic system. They showed in their publication that the proposed system has hidden attractors. Then, they applied it on FPAA to show the accuracy of their proposed system. Yang et al. [29] proposed a new 4-dimensional hyperchaotic system with hidden attractors and existing attractors without an equilibrium point. They performed active control-based synchronization of the proposed system.

Nowadays, secure and effective information communication is increasing and gaining in importance. In this context, chaotic systems and in particular hyperchaotic systems have the potential to offer new and effective solutions for communication security. Recent studies have underscored the challenges in synchronizing hyperchaotic systems, particularly in practical applications involving parameter uncertainty. In systems with parameter uncertainty, achieving synchronization is notably challenging. To address this difficulty, the use of adaptive-based observers is considered a viable solution for designing such systems.

The innovations presented in this study and the contributions of this work to the literature are listed as follows:

- First, a new hyperchaotic system is proposed as an addition to the literature. Comprehensive dynamic analysis of the system is carried out. As a result of the dynamic analysis, it is observed that the proposed system exhibits hyperchaotic behavior.

- Adaptive observer-based synchronization of the new system is designed. While performing the synchronization, parameter uncertainty is also taken into account. As a result of the design, it is observed that the synchronization errors reach zero in a short time, while at the same time the parameter uncertainty is eliminated.
- The adaptive observer-based synchronization method is tested in a secure communication application where chaotic system synchronization is usually used. The transmitted signal is first masked by the transmitting hyperchaotic system and then transmitted to the receiving hyperchaotic system.
- The analysis shows that the transmitted signal is successfully extracted from the masked signal received by the receiving hyperchaotic system within a short period of time.

In Section 2, the mathematical model of the proposed hyperchaotic system is introduced and the necessary dynamic analysis methods are applied. In Section 3, the circuit simulation is performed. In Section 4, adaptive observer-based synchronization of the new hyperchaotic system is implemented and simulated. In Section 5, the realized synchronization is used in a secure communication application. Section 6 presents the conclusions.

2. Materials and Methods

In this paper, various analyses of the proposed 4-dimensional hyperchaotic system were executed. In order to prove that the new hyperchaotic system exhibits chaotic and hyperchaotic behavior, dynamic analysis studies were carried out. Some of these analyses were performed using the MATLAB platform. The hyperchaotic circuit implementation of the system was created on the Multisim platform. The synchronization of the proposed hyperchaotic system was designed using an adaptive observer. The novel 4-dimensional hyperchaotic system synchronization was tested in a secure communication application and its execution was successfully proved. The block diagram of the material and the method proposed in this paper are given in Figure 1.

2.1. The Proposed 4-Dimensional Hyperchaotic System

The mathematical model of the proposed hyperchaotic system is shown in (1):

$$\begin{aligned} \dot{x}_1 &= -12x_1 + 30x_2 \\ \dot{x}_2 &= bx_1 - x_2 - x_1x_3 \\ \dot{x}_3 &= ax_2 + x_1x_2 - x_3 + x_4 \\ \dot{x}_4 &= -x_1b + x_1x_3 - 2x_4 \end{aligned} \tag{1}$$

In the system (1), the variables x_1, x_2, x_3 and x_4 represent states, while a and b are positive parameters. The system (1) demonstrates chaotic behavior for specific values of tuned parameters and the initial conditions that are provided. Notably, the system is distinguished by its independence from the initial conditions. The examination of various initial conditions reveals that under specific parameter values, the system can manifest chaotic, hyperchaotic, periodic and quasi-periodic behaviors.

2.2. Dynamic Analysis of the Proposed Hyperchaotic System

The bifurcation diagram of the proposed new hyperchaotic system is shown in Figure 2. While plotting the bifurcation diagram, the parameter b is taken as 45 and the variation in the parameter a between 14 and 16 is plotted. For the bifurcation diagram analysis, the initial values of the system are taken as $x_1(0) = 1,\ x_2(0) = 1,\ x_3(0) = 1,\ x_4(0) = 1$.

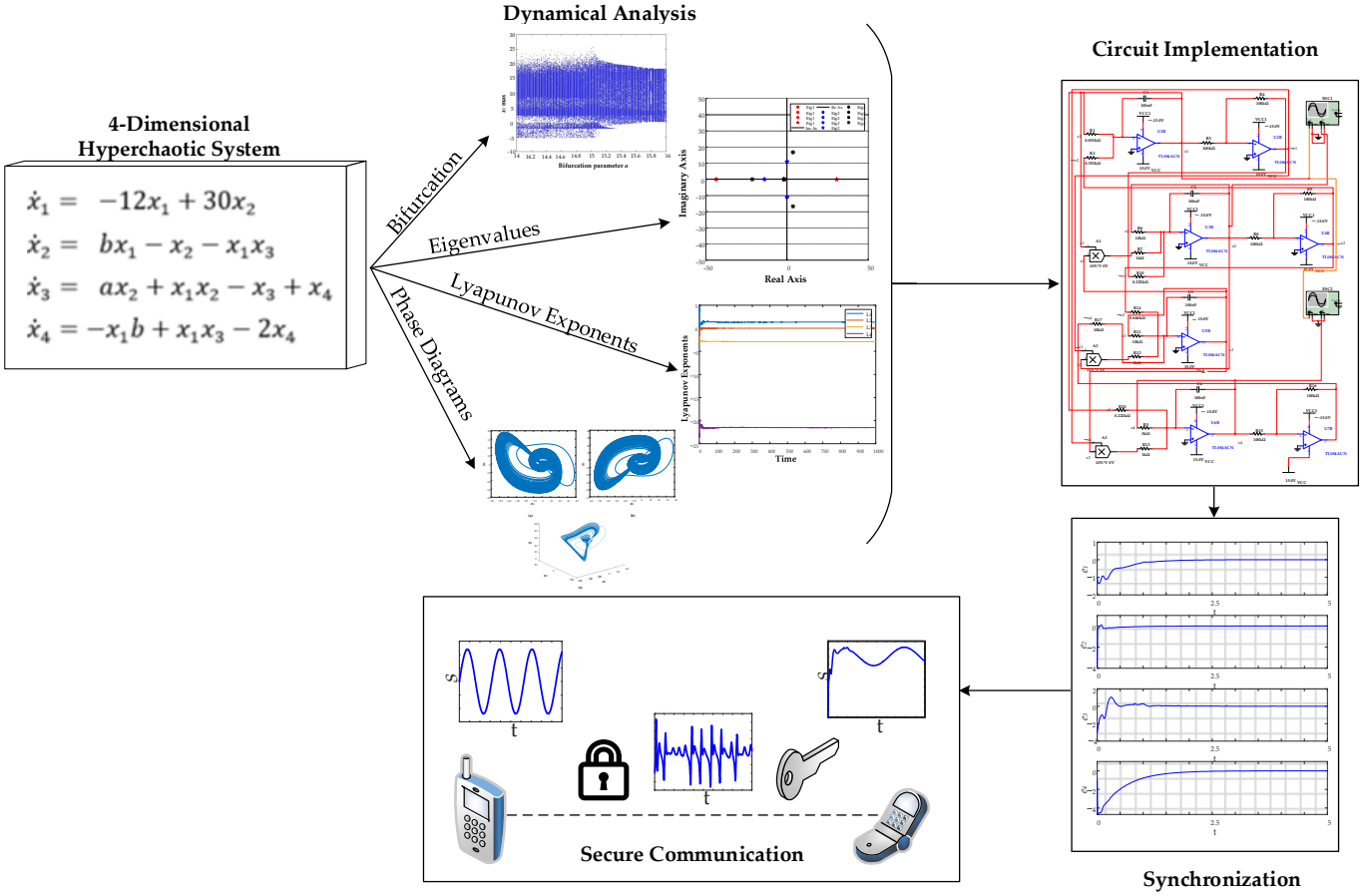

Figure 1. Illustration of the proposed methods.

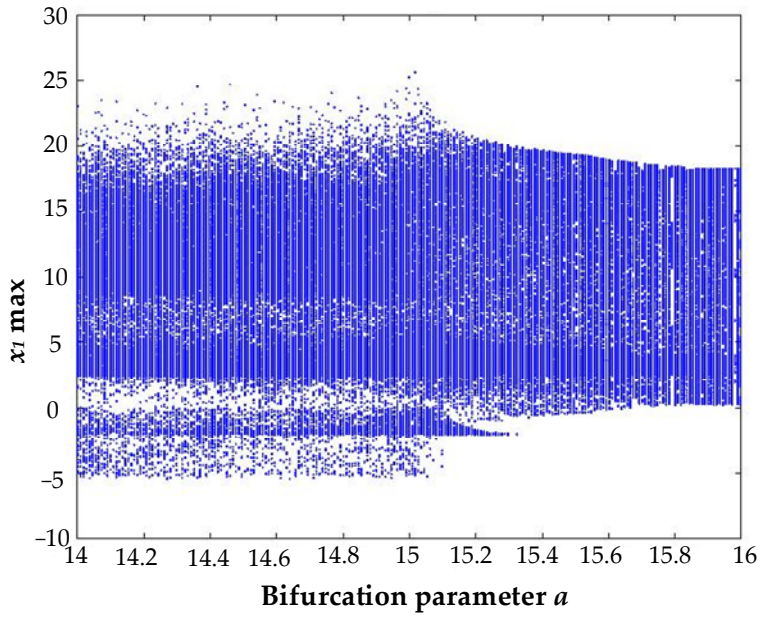

Figure 2. Bifurcation diagram based on a parameter.

As can be seen from the Figure 2, the value of the parameter a is taken as 15 for the proposed system.

Additionally, the 3D bifurcation diagram of the proposed hyperchaotic system is shown in Figure 3. While drawing this bifurcation diagram, in addition to parameter a,

parameter b was also assumed to be between 40 and 50. For the bifurcation diagram analysis, the initial values of the system are taken as $x_1(0) = 1,\ x_2(0) = 1,\ \ x_3(0) = 1,\ \ x_4(0) = 1$.

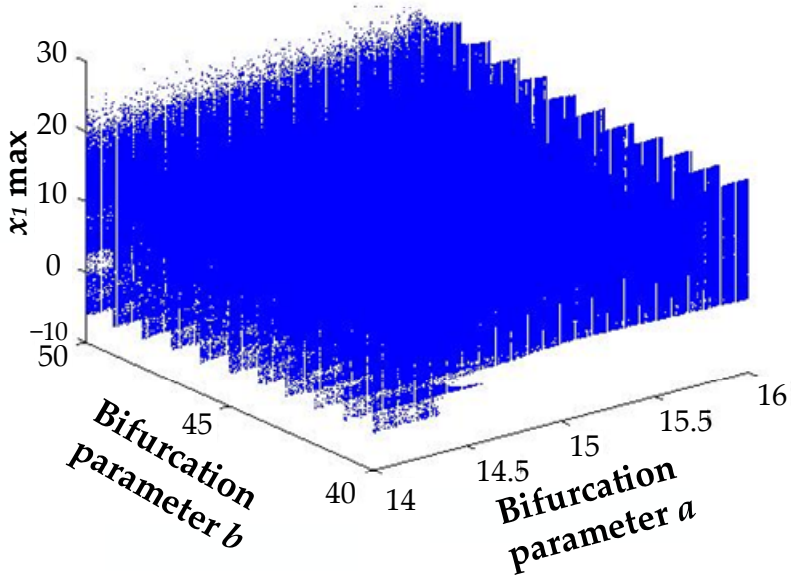

Figure 3. The 3D Bifurcation diagram based on a and b parameters.

Based on Figure 3, the b parameter value of the proposed hyperchaotic system is taken as 45.

The proposed hyperchaotic system can be represented in vector notation as in (2):

$$\dot{x} = f(x) = \begin{bmatrix} f_1(x) \\ f_2(x) \\ f_3(x) \\ f_4(x) \end{bmatrix} \tag{2}$$

Based on this, the proposed system can be expressed as in (3):

$$\begin{aligned} f_1(x) &= -12x_1 + 30x_2 \\ f_2(x) &= bx_1 - x_2 - x_1x_3 \\ f_3(x) &= ax_2 + x_1x_2 - x_3 + x_4 \\ f_4(x) &= -x_1b + x_1x_3 - 2x_4 \end{aligned} \tag{3}$$

The divergence of the hyperchaotic system is investigated as (4) for the system [30]:

$$div\ f = \frac{\partial f_1(x)}{\partial x_1} + \frac{\partial f_2(x)}{\partial x_2} + \frac{\partial f_3(x)}{\partial x_3} + \frac{\partial f_4(x)}{\partial x_4} = -12 - 1 - 1 - 2 = -16 \tag{4}$$

For the divergence of the system, $div\ f < 0$ is required. As can be seen from (4), the system satisfies the condition.

To find the equilibrium points of the proposed hyperchaotic system, the system of equations must be equal to zero. This equality is shown in (5):

$$\begin{aligned} 0 &= -12x_1 + 30x_2 \\ 0 &= bx_1 - x_2 - x_1x_3 \\ 0 &= ax_2 + x_1x_2 - x_3 + x_4 \\ 0 &= -x_1b + x_1x_3 - 2x_4 \end{aligned} \tag{5}$$

When analyzing the bifurcation diagrams of the system, specific values of $a = 15$ and $b = 45$ were chosen to induce hyperchaotic behavior. Under these parameter settings, the system exhibits three equilibrium points, namely $E_1 = [0, 0, 0, 0, 0]$, $E_2 =$

$[5.55, 2.22, 44.6, -1.11]$ and $E_3 = [-20.05, -8.02, 44.6, 4.01]$. To ascertain the stability of the hyperchaotic system, it is imperative to determine the system's eigenvalues. For the specified values $a = 15$ and $b = 45$, the system's Jacobian matrix, essential for calculating the eigenvalues, is presented in (6).

$$J = \begin{bmatrix} -12 & 30 & 0 & 0 \\ b - x_3 & -1 & -x_1 & 0 \\ x_2 & x_1 + a & -1 & 1 \\ x_3 - b & 0 & x_1 & -2 \end{bmatrix} \tag{6}$$

The Jacobian matrix was solved, and the eigenvalues corresponding to the equilibrium points E_1, E_2 and E_3 were determined. Equation (7) was employed for the computation of these eigenvalues:

$$|J - \lambda I| = 0 \tag{7}$$

Table 1 provides the values of the equilibrium points and eigenvalues.

Table 1. Eigenvalues of the system and equilibrium points.

E_i	Equilibrium Points	Eigenvalues
E_1	$[0, 0, 0, 0]$	$(-2.0, -1.0, -43.65, 30.65)$
E_2	$[5.55, 2.22, 44.6, -1.11]$	$(-0.0252 \pm j10.98, -2.03, -13.91)$
E_3	$[-20.05, -8.02, 44.6, 4.01]$	$(3.68 \pm j16.71, -1.96, -21.40)$

The graph of the changes in the eigenvalues of the system is given in Figure 4.

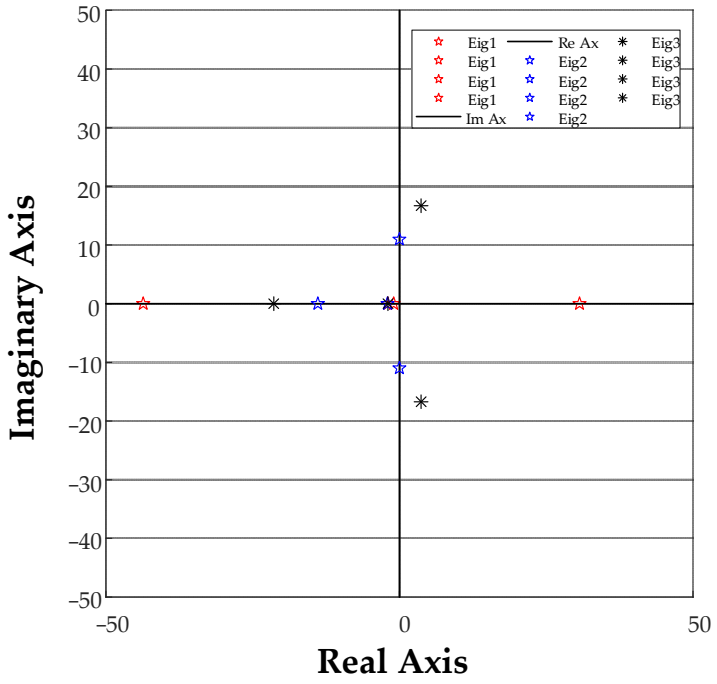

Figure 4. Eigenvalues (λ) of the hyperchaotic system.

Upon analyzing the eigenvalues (λ) of the system, it becomes evident that the system possesses positive eigenvalues, indicating its instability. Furthermore, it can be inferred that the hyperchaotic attractor of the new system is affiliated with the self-exciting family.

The Alan Wolf algorithm was employed for the computation of Lyapunov exponents [31]. For the first computation, throughout the calculation, the initial conditions were set as $x_1(0) = 1$, $x_2(0) = 1$, $x_3(0) = 1$, $x_4(0) = 1$, parameter b was taken as 45

and parameter a was assumed to vary between 14 and 16. The evolution of Lyapunov exponents according to the variation in a parameter is shown in Figure 5.

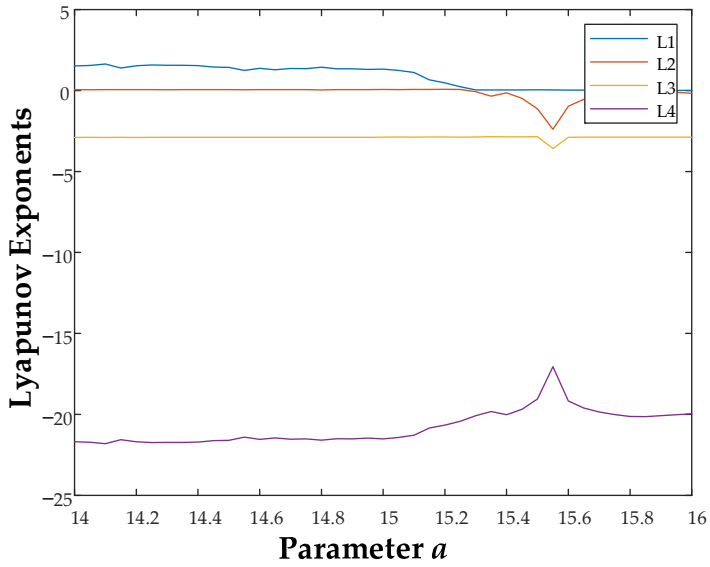

Figure 5. Lyapunov exponents according to the variation in a parameter.

As can be seen from Figure 5, the system has two positive Lyapunov exponent values of a parameter between 14 and 15.3. Therefore, taking the a parameter value of the system as 15 and the b parameter value as 45, the change in the Lyapunov exponents of the system with respect to time is plotted in Figure 6. The initial conditions were set as $x_1(0) = 1$, $x_2(0) = 1$, $x_3(0) = 1$, $x_4(0) = 1$.

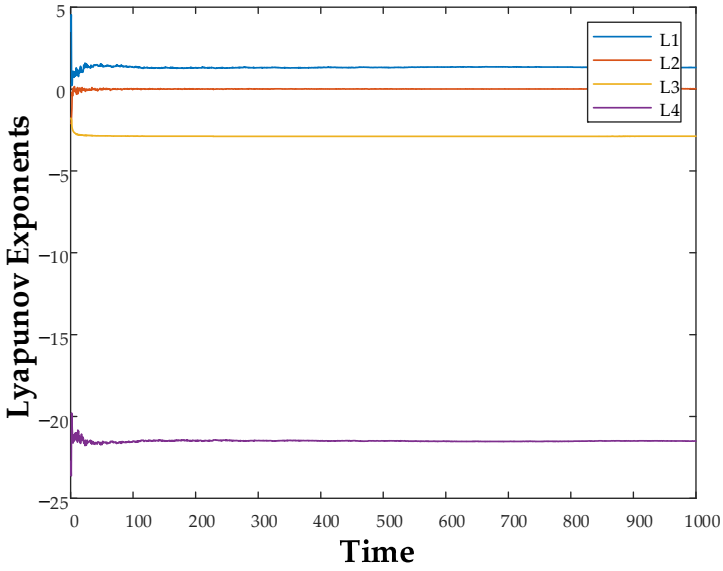

Figure 6. Diagram of Lyapunov exponents of the system.

The Lyapunov exponents are determined as $L_1 = 1.3264$, $L_2 = 0.0227$, $L_3 = -2.8806$ and $L_4 = -21.5094$. Two positive Lyapunov exponents are found when the calculated Lyapunov exponents of the recently suggested hyperchaotic system are examined. As a result, the behavior of the system is hyperchaotic.

Hyperchaotic systems are inevitably drawn to fractals. The degree of system predictability can be inferred from the fractal dimension of the attractor. The data would have been generated by a deterministic system if the fractal dimension is minimal. The

data would have been produced by a random system if the fractal dimension is large. Because this structure is not like other geometrical formations, the researchers use fractal dimensions to explain it [32]. The proposed four-dimensional system exhibits a Lyapunov fractal dimension [33], which is computed using (8):

$$D_{KY} = j + \frac{\sum_{i=1}^{J} L_i}{|L_{j+1}|} = 3 + \frac{1.3264 + 0.0227 - 2.8806}{|-21.5094|} = 2.92 \quad (8)$$

This shows that the proposed system's Lyapunov dimension is fractional. The new system contains non-periodic orbits and close paths that diverge due to its fractal character. As a result, this nonlinear system is truly chaotic.

In engineering applications, chaotic phase behavior can pose challenges in terms of control and predictability. Systems exhibiting chaotic dynamics may be more difficult to control, as small changes in input or conditions can lead to unpredictable outcomes. Engineers need to account for and understand chaotic behavior in order to design robust and reliable systems. The phase space diagrams of the proposed hyperchaotic system in various dimensions are shown in Figure 7. For the phase diagram analysis, $a = 15$, $b = 45$ and the initial values of the system are taken as $x_1(0) = 1,\ x_2(0) = 1,\ x_3(0) = 1,\ x_4(0) = 1$.

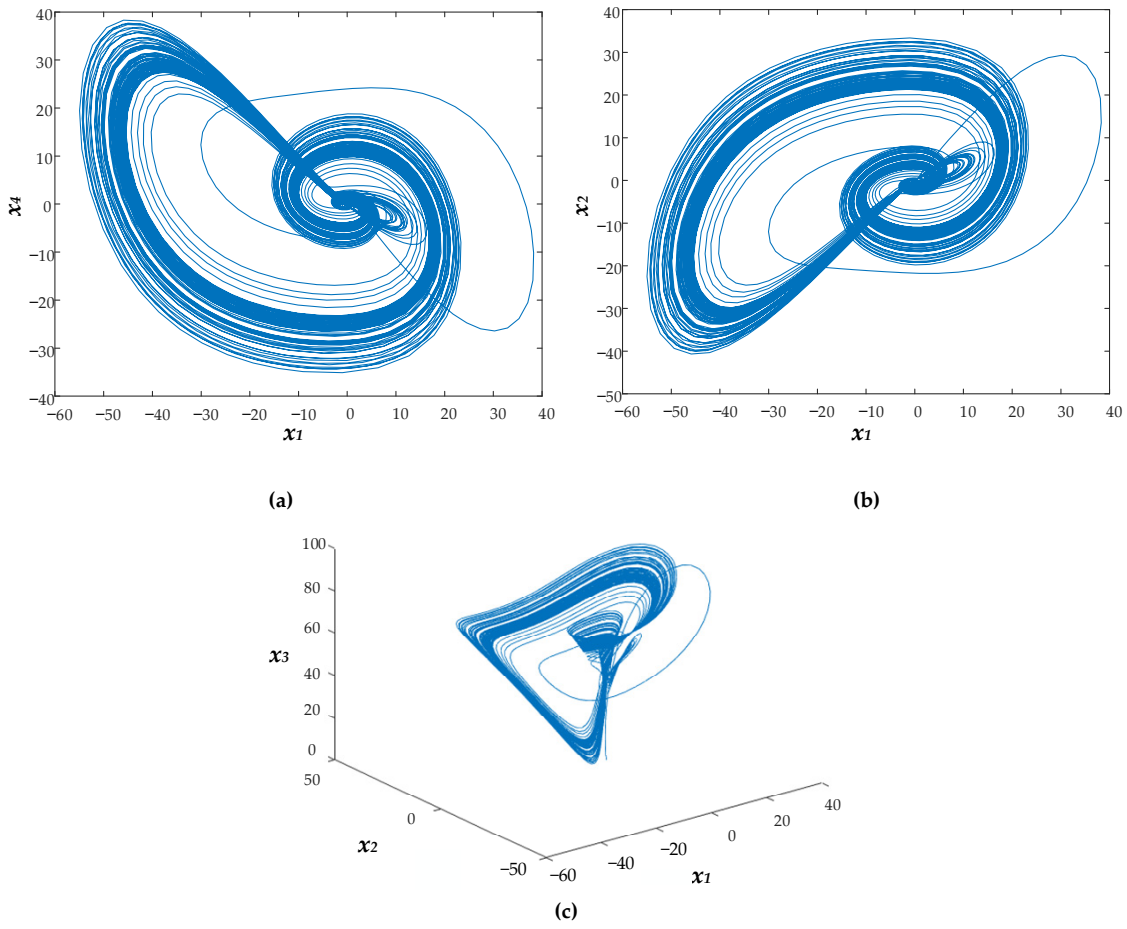

Figure 7. (**a**) x_1 x_4 phase diagram; (**b**) x_1 x_2 phase diagram; (**c**) x_1 x_2 x_3 phase diagram.

The system's phase diagrams reveal that it is a hyperchaotic system with dynamic oscillations and a variety of strange attractors. The phase diagrams for different a and b parameter values are shown in Figure 8. For the phase diagram analysis, $a = 5$ and $b = 6$ values were taken and initial values taken as $x_1(0) = 1,\ x_2(0) = 1,\ \ x_3(0) = 1,\ x_4(0) = 1$.

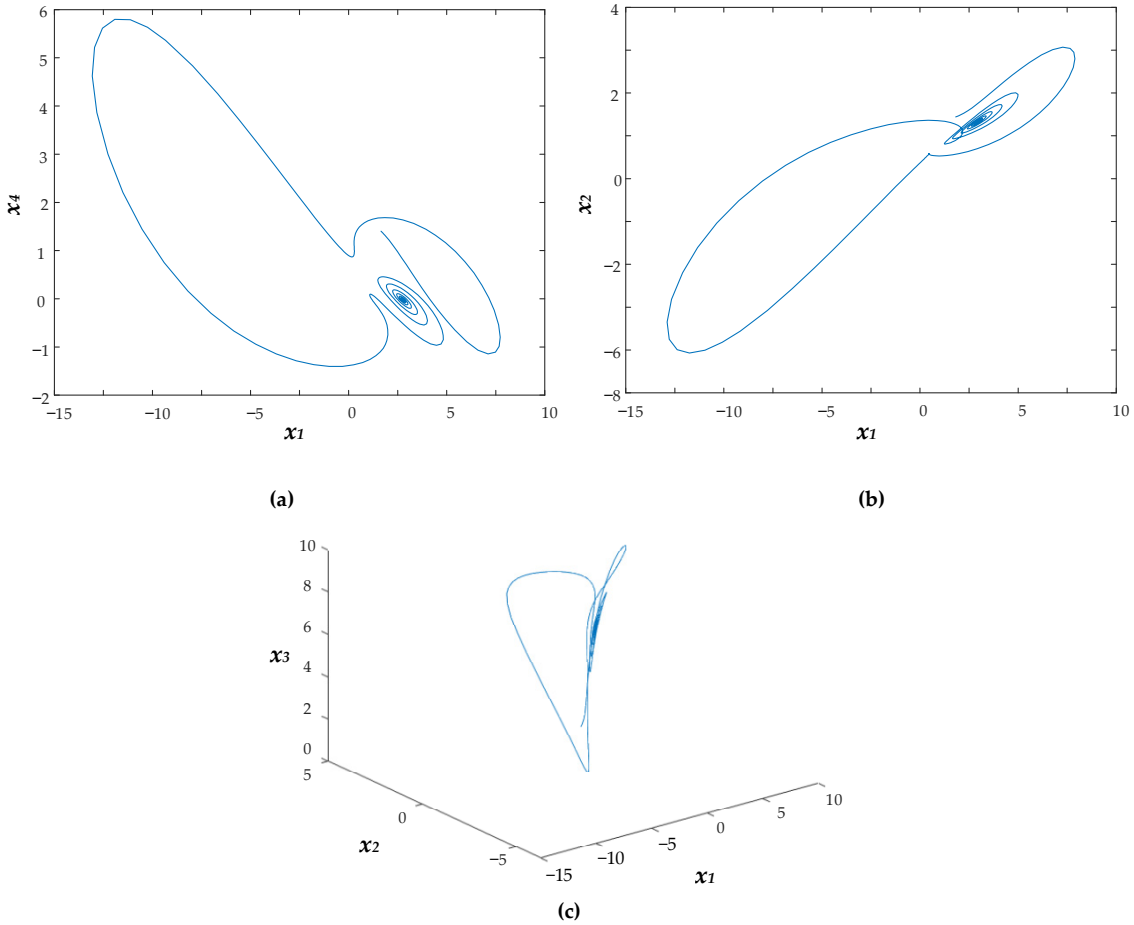

Figure 8. (**a**) x_1 x_4 phase diagram; (**b**) x_1 x_2 phase diagram; (**c**) x_1 x_2 x_3 phase diagram.

As can be seen from Figure 8, the chaotic properties of the system change for different parameter values.

3. Circuit Implementation of the Proposed Hyperchaotic System

Using Multisim 14.3 software, an analogous electronic circuit for the novel hyperchaotic system was created in order to evaluate the viability of the proposed system. The highly visual modeling environment offered by the electronic circuit simulation program Multisim is designed for hyperchaotic systems [34]. It makes the process of creating and fine-tuning circuit models easier and permits the monitoring of their behavior in real time. This real-time feedback forms the basis for simulating the implementation of hyperchaotic systems in embedded circuitry and helps to understand their dynamic features.

For simulating electronic circuits, a variety of software packages are available, including PSPICE 9.2, LTSPICE 17.1.15, Multisim 14.3 and Matlab Simulink 2021a. Multisim, the industry-standard circuit design and simulation program for analog, digital and power electronics in academic and research settings, was chosen for this thesis [35].

An operational amplifier (TL084ACN), a multiplier (IC AD633), linear resistors and capacitors driven by a ±15 V power source are all included in the developed circuit in this thesis. The operational amplifier adds, subtracts and integrates the circuits, and the multiplier, which combines the four state variables into a single cohesive unit, symbolizes the nonlinearity of the system. The system (1) presents the hyperchaotic system from which the electrical circuit equations are obtained, and (9) formulates it:

$$\begin{aligned}
\dot{x}_1 &= \frac{1}{C_1}\left[\frac{1}{R_1}x_1 + \frac{1}{R_2}\left(\frac{R_9}{R_8}\right)(-x_2)\right] \\
\dot{x}_2 &= \frac{1}{C_2}\left[\frac{1}{R_{10}}\left(\frac{R_4}{R_3}\right)(-x_1) + \frac{1}{R_6}x_2 + \frac{1}{R_7}\frac{x_1x_3}{10}\right] \\
\dot{x}_3 &= \frac{1}{C_3}\left[\frac{1}{R_{14}}\left(\frac{R_9}{R_8}\right)(-x_2) + \frac{1}{R_{12}}\left(\frac{R_4}{R_3}\right)\frac{(-x_1)x_2}{10} + \frac{1}{R_{11}}x_3 + \frac{1}{R_{17}}\left(\frac{R_{16}}{R_{15}}\right)(-x_4)\right] \\
\dot{x}_4 &= \frac{1}{C_4}\left[\frac{1}{R_{20}}x_1 + \frac{1}{R_{13}}\left(\frac{R_4}{R_3}\right)\frac{(-x_1)x_3}{10} + \frac{1}{R_5}x_4\right]
\end{aligned} \tag{9}$$

After performing the necessary calculations, the values of the circuit elements were determined as follows: $R_1 = 0.833$ kΩ, $R_2 = 0.333$ kΩ, $R_3 = R_4 = R_8 = R_9 = R_{15} = R_{16} = 100$ kΩ, $R_5 = 5$ kΩ, $R_6 = R_{11} = R_{17} = 10$ kΩ, $R_7 = R_{12} = R_{13} = 1$ kΩ, $R_{10} = R_{20} = 0.222$ kΩ, $R_{14} = 0.666$ kΩ and $C_1 = C_2 = C_3 = C_4 = 100$ μF. The Multisim model of the circuit is illustrated in Figure 9. The circuit model encompasses seven operational amplifiers (TL084ACN), four capacitors, three multipliers (IC AD633), and eighteen resistors.

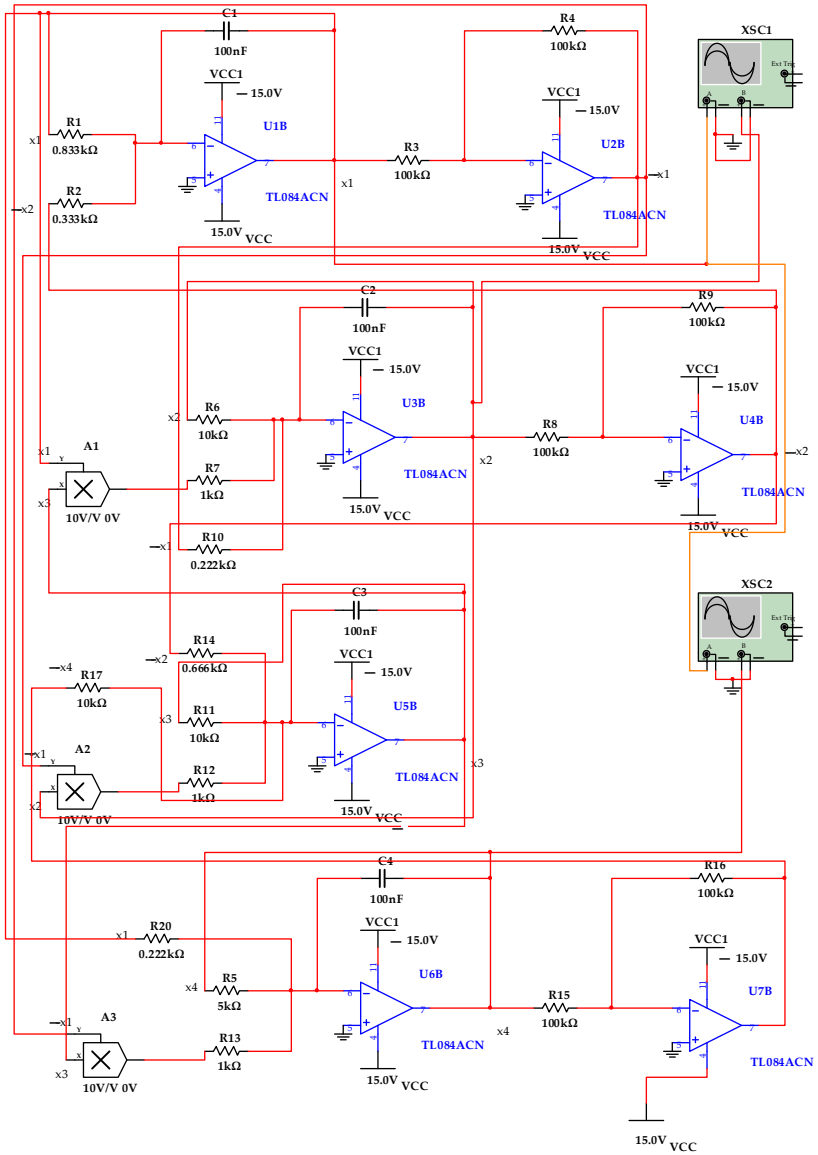

Figure 9. Electronic circuit diagram of the proposed hyperchaotic system.

When the circuit simulation is run, the oscilloscope images showing the phase diagrams of the states are as shown in Figure 10.

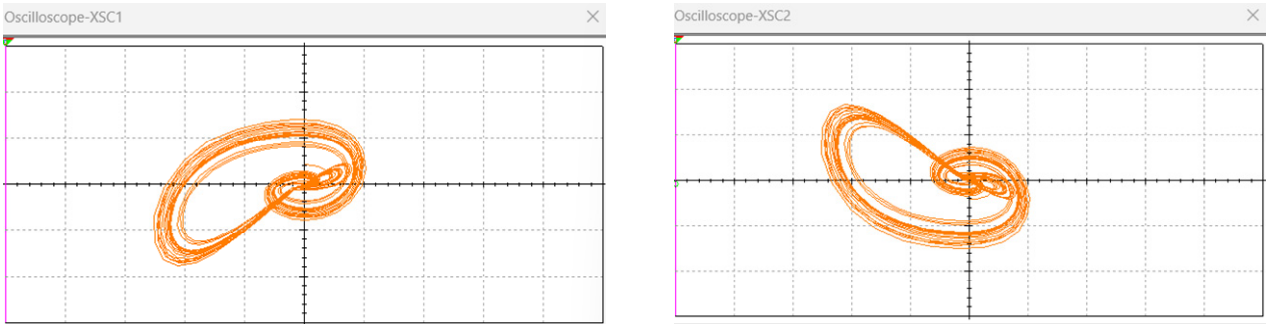

Figure 10. (**a**) Multisim x_1 x_2 phase diagram of the hyperchaotic system; (**b**) Multisim x_1 x_4 phase diagram of the hyperchaotic system.

Similarity was observed between the graphs obtained from the numerical simulation program MATLAB 2021a and the electronic circuit simulation software. Multisim provides a strong confirmation for hyperchaotic attractors. Thoroughly comparing the output data from both software tools shows that there is a significant degree of consistency in the way attractors dynamically behave under different settings and how easily they alter. These results validate the presence of attractors in the hypothesized hyperchaotic system.

Finally, consistency between the electrical circuit simulation findings and numerical simulation results provides a solid theoretical foundation for the actual implementation of the novel hyperchaotic system, while also confirming the feasibility of the system. It provides a strong basis for the application of novel hyperchaotic systems in various domains.

4. Adaptive Observer Based Synchronization of the Proposed Hyperchaotic System

Hyperchaotic systems, which form a separate category within nonlinear systems, are typically characterized by a set of nonlinear differential equations. It is a prevalent practice to decompose a hyperchaotic dynamical system into two components: the linear component and the nonlinear component. In instances where the hyperchaotic dynamical system involves unknown parameters and is influenced by unidentified disturbances, it is often expressed in the form of (10) [36]:

$$\dot{x} = Ax + Bf(x) + Bg(x)\theta + B\eta(x,t) \tag{10}$$

Here, $x \in R^n$ represents the state vector; $\theta \in R^p$ is the vector of unknown parameters; $\eta \in R^r$ is the external disturbance vector; and $A \in R^{nxn}$ and $B \in R^{nxr}$ are known matrices. Additionally, $f(\cdot) \in R^r$ is a nonlinear function vector, and $g(\cdot) \in R^{rxp}$ is a matrix of functions. The matching condition is satisfied by the external disturbance vector, the parameter uncertainty vector and the nonlinear function vector.

It is noteworthy that many hyperchaotic systems can be reformulated into the same structure as (10). For instance, the Lorenz hyperchaotic system can be expressed in the form of (11):

$$\begin{bmatrix} \dot{x}_1 \\ \dot{x}_2 \\ \dot{x}_3 \\ \dot{x}_4 \end{bmatrix} = \begin{bmatrix} -a & a & 0 & 1 \\ 0 & -1 & 0 & 0 \\ 0 & 0 & 0 & 0 \\ 0 & 0 & 0 & r \end{bmatrix} \begin{bmatrix} x_1 \\ x_2 \\ x_3 \\ x_4 \end{bmatrix} + \begin{bmatrix} 0 & 0 & 0 \\ -1 & 0 & 0 \\ 0 & 1 & 0 \\ 0 & -1 & 0 \end{bmatrix} \begin{bmatrix} x_1x_3 \\ x_1x_2 \\ x_2x_3 \end{bmatrix} + \begin{bmatrix} 0 & 0 & 0 \\ -1 & 0 & 0 \\ 0 & 1 & 0 \\ 0 & -1 & 0 \end{bmatrix} \begin{bmatrix} -x_1 & 0 \\ 0 & -x_3 \\ 0 & 0 \end{bmatrix} \begin{bmatrix} c \\ b \end{bmatrix} \tag{11}$$

Here, a is known but c and b are unknown.

We tackle the synchronization challenge of (10) employing the driver–response configuration. In this setup, if the system represented by (10) is designated as the drive system, a corresponding response system needs to be formulated to synchronize with the drive system using a designated driving signal. To achieve this, certain essential assumptions must be fulfilled.

Firstly, the Lipschitz condition is articulated. It is required that the nonlinear function vector $f(x)$ and the matrix $g(x)$ adhere to the Lipschitz condition:

$$\begin{aligned} ||f(x) - f(\hat{x})|| &\leq k_f||x - \hat{x}|| \\ ||g(x) - g(\hat{x})|| &\leq k_g||x - \hat{x}|| \end{aligned} \tag{12}$$

Here, the Lipschitz constants k_f and k_g are considered unknown.

Secondly, the uncertain parameter θ and the external disturbance η are subject to norm bounds defined by two unknown positive constants, denoted as δ_θ and δ_η, respectively.

Thirdly, in pursuit of the objective of hyperchaotic synchronization, it is typically necessary to design artificial output information.

The initial step involves determining a matrix $C_1 \in \Re^{1xn}$ such that the matrix (C_1, A) is observable, and there exists a matrix L such that the Lyapunov equation $(A - LC_1)^T P + P(A - LC_1) = -Q$ has a positive definite matrix solution P for a given positive definite matrix Q.

The second step is to specify $B^T P = C_2$. If there exists a matrix $H \in \Re^{rxp}$ such that $C_2 = HC_1$, then the output matrix of the drive system must be $C = C_1$; otherwise, it will be $C = \left(C_1^T \; C_2^T\right)^T$. In our study, we assume the absence of such an H matrix. Therefore, we set our system output as $y = \left(y_1^T \; y_2^T\right)^T = \left(C_1^T \; C_2^T\right)^T x$.

To synchronize the system presented in (8), an adaptive observer-based response system is designed. This design is illustrated in (11):

$$\dot{\hat{x}} = A\hat{x} + Bf(\hat{x}) + Bg(\hat{x})\hat{\theta} + \frac{1}{2}\bar{k}B(y_2 - C_2\hat{x}) + L(y_1 - C_1\hat{x}) + \alpha(t) \tag{13}$$

Here, $\hat{\theta}$ and $\bar{k}$ symbolize the answers to two adaptation laws that are still to be found, and $\alpha(t)$ is a further control rule that will be defined later [37]. The error signals are $e = x - \hat{x}$, $\widetilde{\theta} = \theta - \hat{\theta}$ and $\widetilde{k} = k - \bar{k}$. Here, k is a constant to be determined. Utilizing (10) and (13), the error dynamics are expressed as follows:

$$\dot{e} = (A - LC_1)e + B(f(x) - f(\hat{x})) + B(g(x)\theta - g(\hat{x})\hat{\theta}) - \frac{1}{2}\bar{k}B(y_2 - C_2\hat{x}) + B\eta - \alpha \tag{14}$$

The synchronization problem thus transforms into ensuring the stability of the error dynamics. The response system can achieve global synchronization with the drive system if it attains global stability at the origin.

We assume the validity of the assumptions for both the driver system and the response system. The response system can synchronize with the driver system under certain conditions.

Firstly, the adaptation laws for $\hat{\theta}$ and $\bar{k}$ are selected as given in (15) and (16):

$$\dot{\hat{\theta}} = l_\theta g(\hat{x})^T (y_2 - C_2\hat{x}) \tag{15}$$

$$\dot{\bar{k}} = l_k \|y_2 - C_2\hat{x}\|^2 \tag{16}$$

Here, the positive constants l_θ and l_k are chosen appropriately.

The additional control law $\alpha(t)$ is chosen as (17):

$$\alpha(t) = r(t)B(y_2 - C_2\hat{x}) \tag{17}$$

The value of $r(t)$ used in (17) is shown in (18):

$$r(t) \geq \frac{\varepsilon_\eta}{2(y_2 - C_2\hat{x})^T} \tag{18}$$

Building upon Assumption 3 and the Kalman and Yakubovich Lemma, two positive definite matrices, denoted as $P = P^T$ and $Q = Q^T$ [38], are introduced. These matrices are considered valid for the algebraic equation.

$$(A - LC_1)^T P + P(A - LC_1) = -Q, \quad B^T P = C_2 \tag{19}$$

To prove the stability of the error dynamics given in (14), let us consider the Lyapunov function candidate given in (20):

$$V = e^T P e + \frac{1}{2} l_k^{-1} \tilde{k}^2 + \frac{1}{l_\theta} \tilde{\theta}^2 \tag{20}$$

The derivative of (20) with respect to time becomes (21):

$$\begin{aligned} \dot{V} = \; & e^T \Big[(A - LC_1)^T P + P(A - LC_1) \Big] e + l_k^{-1} \tilde{k} \dot{\tilde{k}} + \tfrac{2}{l_\theta} \tilde{\theta}^T \dot{\tilde{\theta}} + 2e^T PB(f(x) - f(\hat{x})) \\ & + 2e^T PB\eta - 2e^T P\alpha + 2e^T PB\big(g(x)\theta - g(\hat{x})\hat{\theta}\big) - \bar{k} e^T PB(y_2 - C_2\hat{x}) \end{aligned} \tag{21}$$

If we then rewrite Equation (21) taking into account the law of adaptation given in (15), we obtain (22):

$$\begin{aligned} \dot{V} = \; & -e^T Q e + l_k^{-1} \tilde{k} \dot{\tilde{k}} + 2e^T C_2^T (f(x) - f(\hat{x})) - \bar{k} e^T C_2^T C_2 e + 2e^T C_2^T \eta - 2e^T P\alpha \\ & + 2e^T C_2^T (g(x)\theta - g(\hat{x})\theta) \end{aligned} \tag{22}$$

Given the first assumption, we obtain the inequalities shown in (23):

$$\begin{aligned} & 2e^T C_2^T (f(x) - f(\hat{x})) \leq 2k_f \|C_2 e\| \cdot \|x - \hat{x}\| \leq \tfrac{k_f^2}{\varepsilon_f} \|C_2 e\|^2 + \varepsilon_f \|e\|^2 \\ & 2e^T C_2^T (g(x)\theta - g(\hat{x})\theta) \leq 2k_g \delta_\theta \|C_2 e\| \cdot \|e\| \leq \tfrac{k_g^2 \delta_\theta^2}{\varepsilon_g} \|C_2 e\|^2 + \varepsilon_g \|e\|^2 \\ & 2e^T C_2^T \eta \leq 2\delta_\eta \|C_2 e\| \leq \tfrac{\delta_\eta^2}{\varepsilon_\eta} \|C_2 e\|^2 + \varepsilon_\eta \end{aligned} \tag{23}$$

Here, ε_f, ε_g and ε_η are three appropriate positive constants. Equation (24) is then obtained:

$$\begin{aligned} \dot{V} \leq \; & e^T \Big[(A - LC_1)^T P + P(A - LC_1) + \varepsilon_f I_n + \varepsilon_g I_n \Big] e + l_k^{-1} \tilde{k} \dot{\tilde{k}} \\ & + \left(\tfrac{k_f^2}{\varepsilon_f} + \tfrac{k_g^2 \delta_\theta^2}{\varepsilon_g} + \tfrac{\delta_\eta^2}{\varepsilon_\eta} \right) \|C_2 e\|^2 - \bar{k} \|C_2 e\|^2 + \varepsilon_\eta - 2e^T P\alpha \\ k = \; & \left(\tfrac{k_f^2}{\varepsilon_f} + \tfrac{k_g^2 \delta_\theta^2}{\varepsilon_g} + \tfrac{\delta_\eta^2}{\varepsilon_\eta} \right) \end{aligned} \tag{24}$$

If we modify (24) with the adaptation law given in (15) and the control law given in (17), we obtain (25):

$$\dot{V} \leq e^T \Big[(A - LC)^T P + P(A - LC) + \varepsilon_f I_n + \varepsilon_g I_n \Big] e \tag{25}$$

From the inequality provided in (25), it can be deduced that the independent parameters ε_f and ε_g can be chosen to be sufficiently small, ensuring $\dot{V} < 0$ for all non-zero states. Consequently, the error dynamics presented in (14) can achieve asymptotic stability. In

other words, the drive system given in (10) and the response system given in (13) can be synchronized.

In (24), not only the unknown Lipschitz constants k_f and k_g, but also the unknown limits δ_θ and δ_η can be encompassed within the constant k, which can be adaptively tuned by the adaptation law provided in (16). Moreover, if the constants ε_f and ε_g are chosen to be sufficiently small, the stability of the error dynamics in (14) can be guaranteed.

The initial concept of the control law can be traced back to the work by Guv and Poon [39]. Evidently, as the error $y - C\hat{x}$ approaches zero, the magnitude of $\alpha(t)$ will escalate indefinitely and render computational feasibility unattainable. In practical applications, we can substitute the control law $r(t)$ with (26):

$$\begin{aligned} r(t) &\geq \frac{\varepsilon_\eta}{2\|y_2 - C_2\hat{x}\|^2} \qquad \text{if } \|e\| \geq \varepsilon \\ r(t) &= 0 \qquad\qquad\qquad\quad \text{if } \|e\| < \varepsilon \end{aligned} \tag{26}$$

Here, ε is a sufficiently small positive constant [39]. Consequently, the state error will remain within a neighborhood of the origin.

Hua et al. [40] first proposed the idea of adaptation for unknown Lipschitz constants in order to manage chaotic systems. We expand on this idea in this thesis to synchronize a larger class of hyperchaotic systems that have external disturbances and parameter uncertainty. A control rule can be used to achieve synchronization if the hyperchaotic systems meet the rigorous positive real condition.

Numerical Simulation

In this section of the paper, the effectiveness of adaptive observer-based synchronization for the proposed hyperchaotic system will be demonstrated. The dynamics of the hyperchaotic system are depicted in (27):

$$\begin{aligned} \dot{x}_1 &= -12x_1 + 30x_2 \\ \dot{x}_2 &= bx_1 - x_2 - x_1x_3 \\ \dot{x}_3 &= ax_2 + x_1x_2 - x_3 + x_4 \\ \dot{x}_4 &= -x_1b + x_1x_3 - 2x_4 \end{aligned} \tag{27}$$

It is established that the system exhibits hyperchaotic behavior for $a = 15$ and $b = 45$. Let us consider that the parameter b is unknown, and a has a perturbation of $\Delta_a = 0.03\sin(2t)$. The relevant matrices A, B and C for the hyperchaotic system presented in system (27) are provided in (28)–(30):

$$A = \begin{bmatrix} -12 & 30 & 0 & 0 \\ 0 & -1 & 0 & 0 \\ 0 & a & -1 & 1 \\ 0 & 0 & 0 & -2 \end{bmatrix} \tag{28}$$

$$B = \begin{bmatrix} 0 & 0 \\ -1 & 0 \\ 0 & 1 \\ 1 & 0 \end{bmatrix} \tag{29}$$

$$C_1 = \begin{bmatrix} 1 & 1 & 1 & 0 \end{bmatrix} \tag{30}$$

Furthermore, we define $f(x) = \begin{bmatrix} x_1x_3 \\ x_1x_2 \end{bmatrix}$, $g(x) = \begin{bmatrix} -x_1 \\ 0 \end{bmatrix}$ and $\eta(x,t) = \begin{bmatrix} 0 \\ \Delta_a x_2 \end{bmatrix}$. It is evident that the pair (C, A) is observable. Therefore, the gain matrix L is selected as $L = \begin{bmatrix} -3.5107 & 0.1818 & 1.328 & -0.8 \end{bmatrix}^T$ such that the eigenvalues of the matrix $A - LC_1$ are -6, -4, $-2 + i$ and $-2 - i$. Moreover, the symmetric positive definite matrices provided in (31) and (32) satisfy (19):

$$P = \begin{bmatrix} 0.3475 & -0.3392 & 0.3903 & 0.0379 \\ -0.3392 & 120.7581 & 0.2553 & -3.0015 \\ 0.3903 & 0.2553 & 2.2728 & 0.2408 \\ 0.0379 & -3.0015 & 0.2408 & 4.6182 \end{bmatrix} \tag{31}$$

$$Q = \begin{bmatrix} 6.7527 & 4.4022 & 5.7821 & -3.9132 \\ 4.4022 & 305.9790 & -17.9037 & -18.0623 \\ 5.7821 & -17.9037 & 7.5493 & -5.6039 \\ 0.0379 & -18.0623 & -5.6039 & 17.9912 \end{bmatrix} \tag{32}$$

As mentioned before, the adaptive observer-based response system is designed as (33):

$$\begin{bmatrix} \dot{\hat{x}}_1 \\ \dot{\hat{x}}_2 \\ \dot{\hat{x}}_3 \\ \dot{\hat{x}}_4 \end{bmatrix} = \begin{bmatrix} -12 & 30 & 0 & 0 \\ 0 & -1 & 0 & 0 \\ 0 & a & -1 & 1 \\ 0 & 0 & 0 & -2 \end{bmatrix} \begin{bmatrix} \hat{x}_1 \\ \hat{x}_2 \\ \hat{x}_3 \\ \hat{x}_4 \end{bmatrix} + \begin{bmatrix} 0 & 0 \\ -1 & 0 \\ 0 & 1 \\ 1 & 0 \end{bmatrix} \begin{bmatrix} \hat{x}_1\hat{x}_3 \\ \hat{x}_1\hat{x}_2 \end{bmatrix} + \begin{bmatrix} 0 & 0 \\ -1 & 0 \\ 0 & 1 \\ 1 & 0 \end{bmatrix} \begin{bmatrix} -\hat{x}_1 \\ 0 \end{bmatrix} \begin{bmatrix} \hat{b} \end{bmatrix} + \frac{1}{2}\bar{k} \begin{bmatrix} 0 & 0 \\ -1 & 0 \\ 0 & 1 \\ 1 & 0 \end{bmatrix} (y_2 - C_2\hat{x}) + L(y_1 - C_1\hat{x}) + r(t)B(y_2 - C_2\hat{x}) \tag{33}$$

The values of $r(t)$, $\varepsilon_\eta = 1$ and $\varepsilon = 0.01$ used here are related to the inequalities given in (26) and the laws of adaptation on $\hat{b}$ and $\bar{k}$ are (34) and (35):

$$\dot{\hat{b}} = l_b \begin{bmatrix} -\hat{x}_1 \\ 0 \end{bmatrix}^T (y_2 - C_2\hat{x}) \tag{34}$$

$$\dot{\bar{k}} = l_k \|y_2 - C_2\hat{x}\|^2 \tag{35}$$

Here, $l_b = 1$ and $l_k = 1$. The values for the free parameters ε_f and ε_g, as given in (25), are set to 1. As mentioned earlier, $C_2 = \begin{bmatrix} 0.3771 & -123.7596 & -0.0145 & 7.6197 \\ 0.3903 & 0.2553 & 2.2728 & 0.2408 \end{bmatrix}$ based on the equation $B^T P = C_2$.

The initial conditions for the simulation are $x_1(0) = 1, x_2(0) = 1, x_3(0) = 1, x_4(0) = 1$ ve $\hat{x}_1(0) = 2, \hat{x}_2(0) = 5, \hat{x}_3(0) = 4, \hat{x}_4(0) = 2$ and $\hat{b}(0) = 10, \bar{k}(0) = 10$. The synchronization errors are depicted in Figure 11.

As can be seen in Figure 8, the synchronization error quickly goes to 0. Therefore, it can be said that the synchronization is successful. When other studies in the literature are examined, the synchronization speed and robustness have been very successful. The estimated b value after synchronization is shown in Figure 12.

The b parameter is equal to 45, consistent with the value in the drive system. This suggests that the response system can synchronize with the proposed hyperchaotic system, even in the presence of unknown Lipschitz constants on the function matrices and unknown bounds on uncertainties. As can be seen, the designed structure quickly resisted the parameter uncertainty and predicted the required b value. In summary, the proposed adaptive observer-based response system effectively achieves synchronization with the hyperchaotic system.

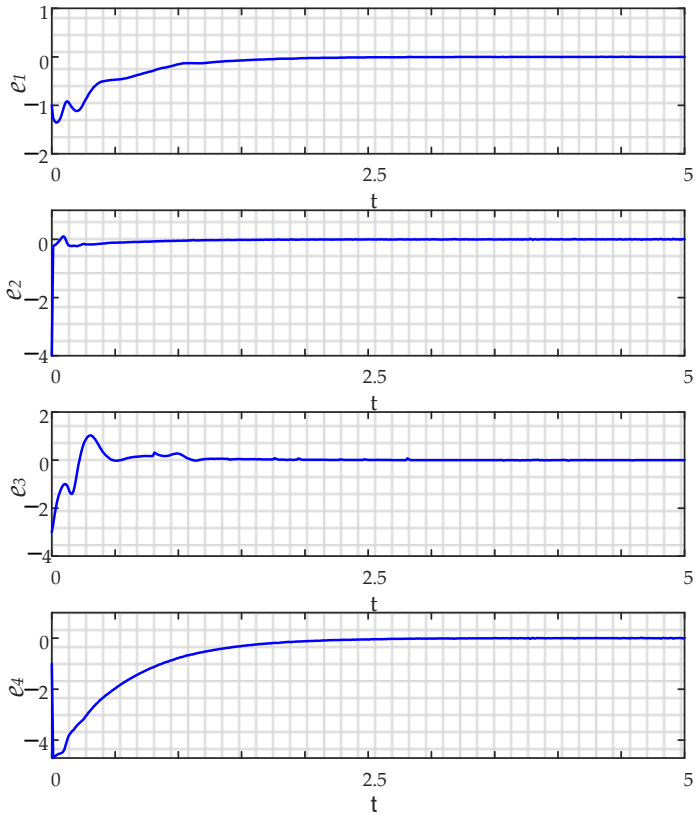

Figure 11. The synchronization errors.

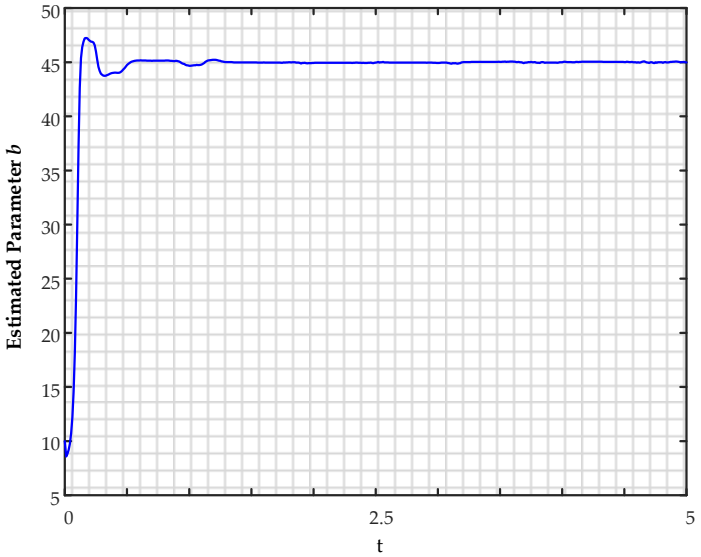

Figure 12. Estimation of unknown parameter b.

5. Application for Secure Communication

In secure communication applications, hyperchaotic synchronization is highly relevant. The simplicity of its implementation in secure communication systems serves as a crucial example of this. The suggested communication system is shown in Figure 13.

At the receiving end of the connection, there is a transmitter (driving) and a receiver (response).

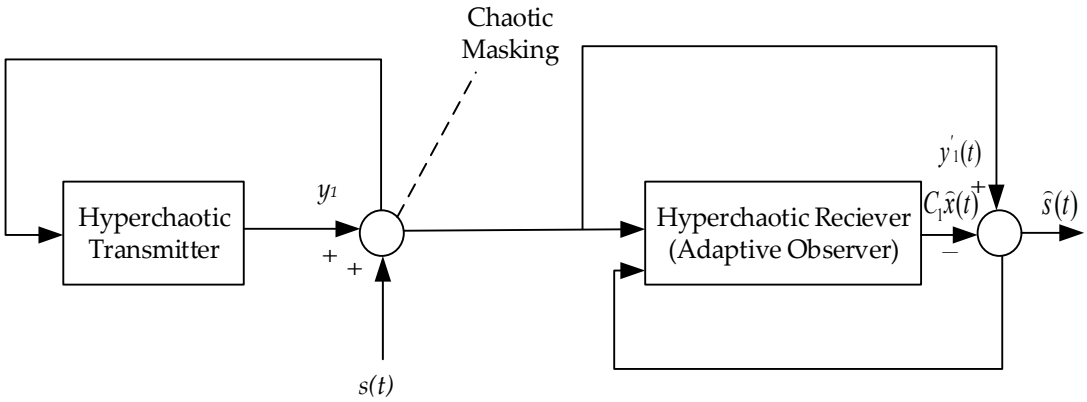

Figure 13. Secure communication system with chaotic masking.

The information signal and the chaotic transmitter's output combine to generate the sent signal. The information is deliberately included into the driving mechanism to create the transmitter. Therefore, the transmitter is the synchronized hyperchaotic system with the additional information signal. The system (36) expresses the used system:

$$\begin{aligned} \dot{x} &= Ax + Bf(x) + Bg(x)\theta + B\eta(x,t) \\ y'_1 &= y_1 + s(t) \end{aligned} \tag{36}$$

Here, $s \in \Re$ represents the information signal and $y'_1(t)$ is one of the transmitted signals guiding the receiver in the hyperchaotic system. Another transmitted signal is formulated as $y'_2 = y_2 = C_2 x$. Following synchronization, the recovery of the information signal $\hat{s}(t)$ can be achieved as detailed in (37):

$$\hat{s}(t) = y'_1(t) - C_1\hat{x}(t) \tag{37}$$

We acknowledge that the error dynamics are governed by (14) during the synchronization design. Therefore, akin to its proof, it is concluded that the transmitter can be synchronized. Upon the completion of synchronization, the following function is attained (38):

$$\lim_{t\to\infty}\hat{s}(t) = \lim_{t\to\infty}\left(y'_1(t) - C_1\hat{x}(t)\right) = \lim_{t\to\infty}\left(C_1x(t) + s(t) - C_1\hat{x}(t)\right) = \lim_{t\to\infty}s(t) \tag{38}$$

This signifies the successful recovery of the information signal. For the simulation, the values employed during synchronization are utilized and $s(t) = 1.2\sin(2t)$ is considered as the information signal. The information signal is depicted and the two transmission signals are formulated as $y'_1(t) = C_1x(t) + s(t)$ and $y'_2 = C_2x$. The information signal $s(t)$, the signal y'_1 masked (i.e., encrypted, with the transmitted information signal) and the $s(t)$ signal obtained after synchronization and the recovery error after secure communication are illustrated in Figure 14.

As can be seen in Figure 14c, the encrypted signal shown in Figure 14b is decrypted by the receiver in a very short time and the information signal is obtained. The simulation results prove that the secure communication design is successful.

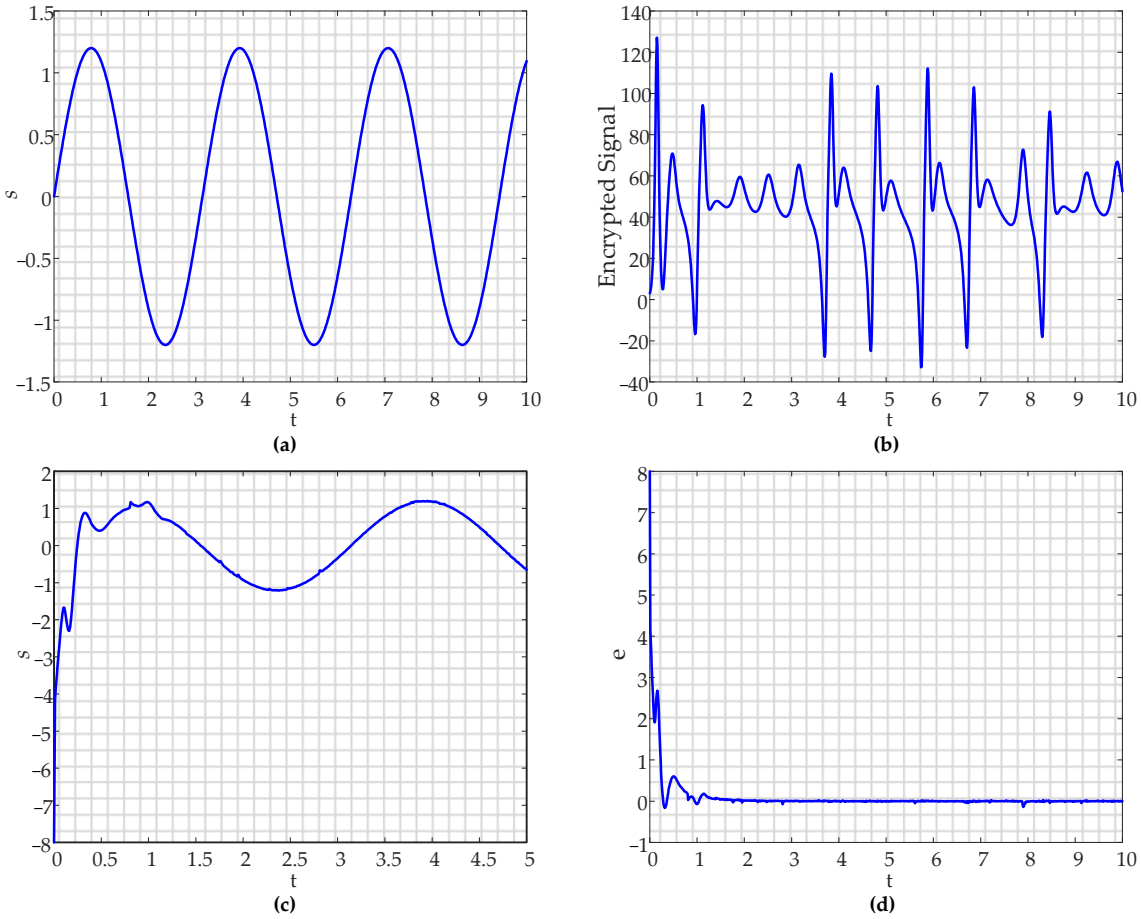

Figure 14. (**a**) Information signal; (**b**) transmitted encrypted signal; (**c**) the signal obtained after synchronization; (**d**) recovery error.

6. Conclusions

Our study addresses current challenges in chaotic systems, specifically focusing on the introduction and analysis of a novel hyperchaotic system. Through dynamic analysis, it is concluded that there is significant hyperchaotic behavior, paving the way for novel applications in secure communication. To validate the physical feasibility of our proposed system, an equivalent electronic circuit (see Figure 9) was created. The success of our adaptive observer-based synchronization under parameter uncertainty demonstrates a robust solution to real-world scenarios. This synchronization method, analyzed through Lyapunov stability theory, showcases its effectiveness by converging the synchronization error to 0 and accurately estimating unknown parameter values. The application of adaptive observer-based hyperchaotic system synchronization to secure communication, employing the chaotic masking method (see Figure 13), adds a layer of practical significance. Our system not only ensures the secure transmission of information but also successfully decodes the masked signal at the receiving end. Our study contributes to the understanding and application of hyperchaotic systems, with notable findings in both theoretical and practical domains. However, it is crucial to acknowledge limitations. While our methodology demonstrates success in simulation, future work should involve implementing the proposed system in hardware-based applications to bridge the gap between simulation and real-world scenarios. In conclusion, our research not only highlights the dynamic properties of the proposed hyperchaotic system but also showcases a synchronization method with promising applications in secure communication. By addressing current challenges, presenting innovative solutions and acknowledging the path forward, we contribute to

the advancement of chaotic systems research and open avenues for future exploration and refinement.

Author Contributions: Conceptualization, E.O. and A.G.; methodology, E.O. and A.G.; validation, A.G.; formal analysis, E.O. and A.G.; investigation, E.O.; simulations, E.O.; writing—original draft preparation, E.O. and A.G.; writing—review and editing, E.O. and A.G.; visualization, E.O.; supervision, A.G. All authors have read and agreed to the published version of the manuscript.

Funding: This research received no external funding.

Institutional Review Board Statement: Not applicable.

Informed Consent Statement: Not applicable.

Data Availability Statement: The original contributions presented in the study are included in the article, further inquiries can be directed to the corresponding author.

Conflicts of Interest: The authors declare no conflicts of interest.

References

1. Kolumban, G.; Kennedy, M.P.; Chua, L.O. The Role of Synchronization in Digital Communications Using Chaos. II. Chaotic Modulation and Chaotic Synchronization. *IEEE Trans. Circuits Syst. I Fundam. Theory Appl.* **1998**, *45*, 1129–1140. [CrossRef]
2. Lorenz, E.N. Deterministic Nonperiodic Flow. *J. Atmos. Sci.* **1963**, *20*, 130–141. [CrossRef]
3. Rossler, O.E. An Equation for Hyperchaos. *Phys. Lett. A* **1979**, *71*, 155–157. [CrossRef]
4. Emiroglu, S.; Akgül, A.; Adıyaman, Y.; Gümüş, T.E.; Uyaroglu, Y.; Yalçın, M.A. A New Hyperchaotic System from T Chaotic System: Dynamical Analysis, Circuit Implementation, Control and Synchronization. *Circuit World* **2022**, *48*, 265–277. [CrossRef]
5. Wei, Z.; Wang, F.; Li, H.; Zhang, W. Jacobi Stability Analysis and Impulsive Control of a 5D Self-Exciting Homopolar Disc Dynamo. *DCDS-B* **2022**, *27*, 5029. [CrossRef]
6. Wei, Z.; Zhang, W.; Moroz, I.; Kuznetsov, N.V. Codimension One and Two Bifurcations in Cattaneo-Christov Heat Flux Model. *Discret. Contin. Dyn. Syst. Ser. B* **2020**, *26*, 5305–5319. [CrossRef]
7. Wei, Z.; Li, Y.; Sang, B.; Liu, Y.; Zhang, W. Complex Dynamical Behaviors in a 3D Simple Chaotic Flow with 3D Stable or 3D Unstable Manifolds of a Single Equilibrium. *Int. J. Bifurc. Chaos* **2019**, *29*, 1950095. [CrossRef]
8. Xue, H.; Du, J.; Li, S.; Ma, W. Region of Interest Encryption for Color Images Based on a Hyperchaotic System with Three Positive Lyapunov Exponets. *Opt. Laser Technol.* **2018**, *106*, 506–516. [CrossRef]
9. Zelinka, I.; Senkerik, R. Chaotic Attractors of Discrete Dynamical Systems Used in the Core of Evolutionary Algorithms: State of Art and Perspectives. *J. Differ. Equ. Appl.* **2023**, *29*, 1202–1227. [CrossRef]
10. Feng, W.; Wang, Q.; Liu, H.; Ren, Y.; Zhang, J.; Zhang, S.; Qian, K.; Wen, H. Exploiting Newly Designed Fractional-Order 3D Lorenz Chaotic System and 2D Discrete Polynomial Hyper-Chaotic Map for High-Performance Multi-Image Encryption. *Fractal Fract.* **2023**, *7*, 887. [CrossRef]
11. Feng, W.; Zhao, X.; Zhang, J.; Qin, Z.; Zhang, J.; He, Y. Image Encryption Algorithm Based on Plane-Level Image Filtering and Discrete Logarithmic Transform. *Mathematics* **2022**, *10*, 2751. [CrossRef]
12. Matsumoto, T.; Chua, L.O.; Kobayashi, K. Hyper Chaos: Laboratory Experiment and Numerical Confirmation. *IEEE Trans. Circuits Syst.* **1986**, *33*, 1143–1147. [CrossRef]
13. Kopp, M. Hyperchaos, Adaptive Control, Synchronization, and Electronic Circuit Design of a Novel 6D Hyperchaotic Convective Dynamo System. *TechRxiv* **2022**. [CrossRef]
14. Yujun, N.; Xingyuan, W.; Mingjun, W.; Huaguang, Z. A New Hyperchaotic System and Its Circuit Implementation. *Commun. Nonlinear Sci. Numer. Simul.* **2010**, *15*, 3518–3524. [CrossRef]
15. Zhang, J.; Hou, J.; Xu, L.; Zhu, X.; Xie, Q. Dynamical Analysis, Circuit Implementation, and Simultaneous Application of a Novel Four-Dimensional Hyperchaotic System Based on Cosine Functions. *Microelectron. Eng.* **2023**, *271–272*, 111939. [CrossRef]
16. Aguilar-Bustos, A.Y.; Cruz-Hernández, C. Synchronization of Discrete-Time Hyperchaotic Systems: An Application in Communications. *Chaos Solitons Fractals* **2009**, *41*, 1301–1310. [CrossRef]
17. Wang, Y.; Xue, Y.; Wang, X.; Ceng, B.-l.; Qiao, Y.-f. Dynamic Behaviors in Two-Layer Coupled Oscillator System. *Chaos Solitons Fractals* **2021**, *144*, 110454. [CrossRef]
18. Pecora, L.M.; Carroll, T.L. Synchronization in Chaotic Systems. *Phys. Rev. Lett.* **1990**, *64*, 821. [CrossRef]
19. Chen, S.; Lü, J. Synchronization of an Uncertain Unified Chaotic System via Adaptive Control. *Chaos Solitons Fractals* **2002**, *14*, 643–647. [CrossRef]
20. Chen, S.; Lü, J. Parameters Identification and Synchronization of Chaotic Systems Based upon Adaptive Control. *Phys. Lett. A* **2002**, *299*, 353–358. [CrossRef]
21. Feki, M.; Robert, B. Observer-Based Chaotic Synchronization in the Presence of Unknown Inputs. *Chaos Solitons Fractals* **2003**, *15*, 831–840. [CrossRef]

22. Zhao, Y.; Zhang, W.; Su, H.; Yang, J. Observer-Based Synchronization of Chaotic Systems Satisfying Incremental Quadratic Constraints and Its Application in Secure Communication. *IEEE Trans. Syst. Man Cybern. Syst.* **2018**, *50*, 5221–5232. [CrossRef]
23. Liao, T.-L.; Tsai, S.-H. Adaptive Synchronization of Chaotic Systems and Its Application to Secure Communications. *Chaos Solitons Fractals* **2000**, *11*, 1387–1396. [CrossRef]
24. Shoreh, A.-H.; Kuznetsov, N.V.; Mokaev, T.N. New Adaptive Synchronization Algorithm for a General Class of Complex Hyperchaotic Systems with Unknown Parameters and Its Application to Secure Communication. *Phys. A Stat. Mech. Its Appl.* **2022**, *586*, 126466. [CrossRef]
25. Wu, X.-J.; Wang, H.; Lu, H.-T. Hyperchaotic Secure Communication via Generalized Function Projective Synchronization. *Nonlinear Anal. Real World Appl.* **2011**, *12*, 1288–1299. [CrossRef]
26. Hassan, M.F. A New Approach for Secure Communication Using Constrained Hyperchaotic Systems. *Appl. Math. Comput.* **2014**, *246*, 711–730. [CrossRef]
27. Xiong, L.; Liu, Z.; Zhang, X. Dynamical Analysis, Synchronization, Circuit Design, and Secure Communication of a Novel Hyperchaotic System. *Complexity* **2017**, *2017*, e4962739. [CrossRef]
28. Iskakova, K.; Alam, M.M.; Ahmad, S.; Saifullah, S.; Akgül, A.; Yılmaz, G. Dynamical Study of a Novel 4D Hyperchaotic System: An Integer and Fractional Order Analysis. *Math. Comput. Simul.* **2023**, *208*, 219–245. [CrossRef]
29. Yang, M.; Dong, C.; Sui, X. A New Four-Dimensional Hyperchaotic System with Hidden Attractors and Multistablity. *Phys. Scr.* **2023**, *98*, 125261. [CrossRef]
30. Shivamoggi, B.K. Chaos in Dissipative Systems. In *Nonlinear Dynamics and Chaotic Phenomena: An Introduction*; Fluid Mechanics and Its Applications; Springer: Dordrecht, The Netherlands, 2014; Volume 103, pp. 189–244. ISBN 978-94-007-7093-5.
31. Wolf, A.; Swift, J.B.; Swinney, H.L.; Vastano, J.A. Determining Lyapunov Exponents from a Time Series. *Phys. D Nonlinear Phenom.* **1985**, *16*, 285–317. [CrossRef]
32. Frederickson, P.; Kaplan, J.L.; Yorke, E.D.; Yorke, J.A. The Liapunov Dimension of Strange Attractors. *J. Differ. Equ.* **1983**, *49*, 185–207. [CrossRef]
33. Kuznetsov, N.V. The Lyapunov Dimension and Its Estimation via the Leonov Method. *Phys. Lett. A* **2016**, *380*, 2142–2149. [CrossRef]
34. Mobayen, S.; Vaidyanathan, S.; Sambas, A.; Kacar, S.; Çavuşoğlu, Ü. A Novel Chaotic System with Boomerang-Shaped Equilibrium, Its Circuit Implementation and Application to Sound Encryption. *Iran. J. Sci. Technol. Trans. Electr. Eng.* **2019**, *43*, 1–12. [CrossRef]
35. Fu, S.; Cheng, X.; Liu, J. Dynamics, Circuit Design, Feedback Control of a New Hyperchaotic System and Its Application in Audio Encryption. *Sci. Rep.* **2023**, *13*, 19385. [CrossRef] [PubMed]
36. Chen, M.; Zhou, D.; Shang, Y. Synchronizing a Class of Uncertain Chaotic Systems. *Phys. Lett. A* **2005**, *337*, 384–390. [CrossRef]
37. Zhu, F. Observer-Based Synchronization of Uncertain Chaotic System and Its Application to Secure Communications. *Chaos Solitons Fractals* **2009**, *40*, 2384–2391. [CrossRef]
38. Ioannou, P.A.; Sun, J. *Robust Adaptive Control*; PTR Prentice-Hall: Upper Saddle River, NJ, USA, 1996; Volume 1.
39. Gu, D.-W.; Poon, F.W. A Robust State Observer Scheme. *IEEE Trans. Autom. Control* **2001**, *46*, 1958–1963.
40. Hua, C.; Guan, X.; Li, X.; Shi, P. Adaptive Observer-Based Control for a Class of Chaotic Systems. *Chaos Solitons Fractals* **2004**, *22*, 103–110. [CrossRef]